



## Communications

## *Anaplasma* pathogen infection alters chemical composition of the exoskeleton of hard ticks (Acari: Ixodidae)



José de la Fuente<sup>a,b,\*</sup>, José Francisco Lima-Barbero<sup>a</sup>, Eduardo Prado<sup>c</sup>, Iván Pacheco<sup>a</sup>, Pilar Alberdi<sup>a</sup>, Margarita Villar<sup>a,1</sup>

<sup>a</sup>SaBio, Instituto de Investigación en Recursos Cinegéticos (IREC-CSIC-UCLM-JCCM), Ronda de Toledo s/n, 13005 Ciudad Real, Spain

<sup>b</sup>Department of Veterinary Pathobiology, Center for Veterinary Health Sciences, Oklahoma State University, Stillwater, OK 74078, USA

<sup>c</sup>Department of Applied Physics, Faculty of Chemical Sciences and Technologies, Universidad de Castilla-La Mancha, Avda. Camilo José Cela 10, 13071 Ciudad Real, Spain

## ARTICLE INFO

## Article history:

Received 14 November 2019

Received in revised form 8 January 2020

Accepted 9 January 2020

Available online 23 January 2020

## Keywords:

Tick

Pathogen

Exoskeleton

Energy dispersive spectroscopy

Structural protein

Elementomics

## ABSTRACT

Ticks are arthropod ectoparasites and vectors of pathogens affecting human and animal health worldwide. The exoskeleton is a structure that protect arthropods from natural threats such as predators and diseases. Both structural proteins and chemical elements are components of the exoskeleton. However, the chemical composition and effect of pathogen infection on tick exoskeleton properties has not been characterized. In this study, we characterized the chemical composition of tick exoskeleton and the effect of *Anaplasma* pathogen infection on the chemical elements of the exoskeleton and selected structural proteins. The chemical composition was characterized ventral, dorsal upper and dorsal lower regions of tick exoskeleton by scanning electron microscopy and energy dispersive spectroscopy and compared between infected and uninfected ticks. The levels of selected structural proteins were analyzed in infected and uninfected *I. scapularis* salivary glands by immunofluorescence analysis. The results showed that tick exoskeleton contains chemical elements also found in other arthropods. Some of the identified elements such as Mg and Al may be involved in tick exoskeleton stabilization through biomineralization of structural proteins that may be overrepresented in response to pathogen infection. These results suggested that pathogen infection alters the chemical composition of tick exoskeleton by mechanisms still to be characterized and with tick species and exoskeleton region-specific differences.

© 2020 The Authors. Published by Elsevier B.V. on behalf of Research Network of Computational and Structural Biotechnology. This is an open access article under the CC BY-NC-ND license (<http://creativecommons.org/licenses/by-nc-nd/4.0/>).

## 1. Introduction

Ticks are arthropod blood-feeding ectoparasites that vector pathogens such as *Anaplasma phagocytophilum* and *Anaplasma marginale* affecting human and animal health worldwide [1,2]. The exoskeleton is a structure that protects arthropods from natural threats such as predators and diseases. In ticks as in other terrestrial arthropods, the relative amount of chitin fibrils and protein matrix, protein composition, pH/water content of the matrix, composition of chemical elements and cross-linking of the matrix protein affect the properties of the exoskeleton [3–7]. It has been shown that mechanical properties of tick cuticle change during tick

feeding to support the increase in body size and mass during this process [3]. However, the impact of pathogen infection on tick exoskeleton properties has not been investigated. Herein, we provided the first characterization of chemical composition of tick exoskeleton and characterized the effect of *Anaplasma* pathogen infection on the chemical composition of the exoskeleton and selected structural proteins in two species of hard ticks, *Ixodes scapularis* (Say, 1821) and *Rhipicephalus microplus* (Canestrini, 1888) (Acari: Ixodidae).

## 2. Results and Discussion

Scanning electron microscopy and energy dispersive spectroscopy were used for the analysis of chemical elements in *I. scapularis* and *R. microplus* exoskeleton and focusing on the comparison between infected and uninfected ticks (Table S1, Data S1). The chemical composition was characterized in tick exoskeleton ventral, dorsal upper and dorsal lower parts (Fig. 1A). The

\* Corresponding author at: SaBio, Instituto de Investigación en Recursos Cinegéticos, Ronda de Toledo s/n, 13005 Ciudad Real, Spain.

E-mail address: [jose.delafuente@yahoo.com](mailto:jose.delafuente@yahoo.com) (J. de la Fuente).

<sup>1</sup> Present address: Biochemistry Section, Faculty of Science and Chemical Technologies, and Regional Centre for Biomedical Research (CRIB), University of Castilla-La Mancha, 13071 Ciudad Real, Spain.

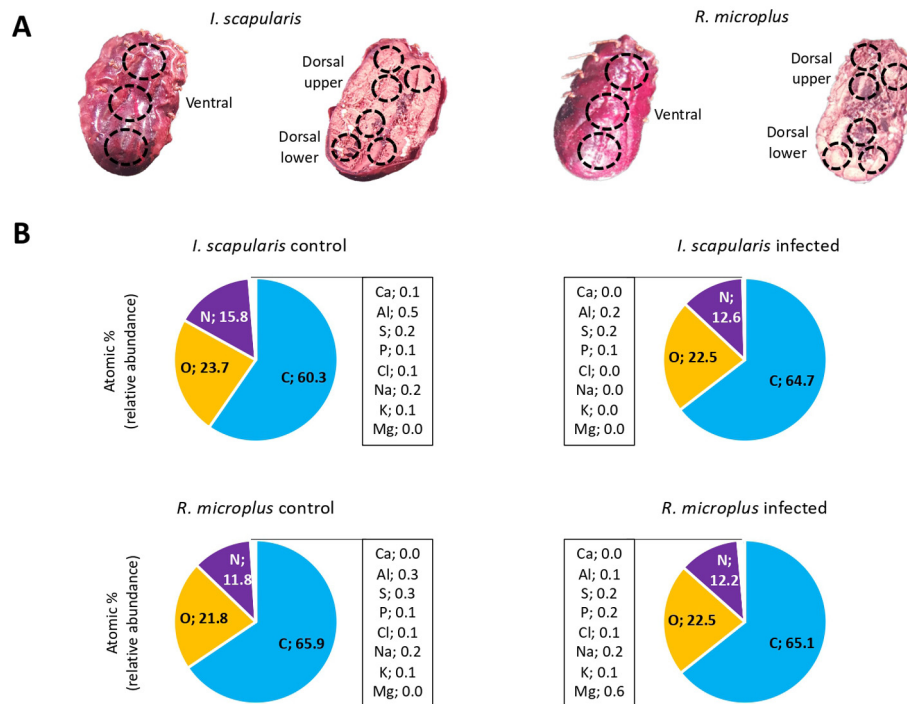


**Fig. 1.** Composition of chemical elements in tick cement. Chemical elements were identified by scanning electron microscopy and energy dispersive spectroscopy analysis in samples from *I. scapularis* and *R. microplus* engorged female ticks. (A) Representative images of analyzed ticks showing the scanning areas on tick exoskeleton ventral, dorsal upper and dorsal lower regions. (B) Representation of the relative abundance of tick exoskeleton most abundant (C, O and N with >10 at.%) and less abundant (<1 at.%) chemical elements based on the average atomic percent for each tick species.

results showed the presence with high relative abundance (>10 at.%) of C, O and N in all regions of the exoskeleton in both tick species (Fig. 1B and Table S1). Other elements with low relative abundance (<1 at.%) such as Al, S, P, Cl, Na and K were present in both tick species but not in all regions (Figs. 1B and 2). However, the elements Ca and Mg were more tick species specific and found only in *I. scapularis* and *R. microplus*, respectively (Figs. 1B and 2). Other elements (Si, Mo, Br) were only rarely found in some samples and were not included in the analysis.

The effect of *Anaplasma* pathogen infection on tick exoskeleton chemical elements was analyzed by comparing composition between infected and uninfected control ticks for each exoskeleton region (Fig. 1A) and considering statistically significant differences only when analysis by both Student's *t*-test with unequal variance and one-way ANOVA test resulted in a *p*-value lower than 0.05 (Fig. 2 and Table S1). The results showed differences between tick species and exoskeleton regions. While the relative abundance for C increased in response to infection in *I. scapularis* ventral and dorsal lower regions, it decreased in *R. microplus* ventral exoskeleton region (Fig. 2). Similarly, O and N relative abundance decreased in *I. scapularis* but increased in *R. microplus* ventral regions in response to infection (Fig. 2). In the *R. microplus* dorsal lower region, the relative abundance of N and S decreased and that of O increased in response to infection (Fig. 2). In the dorsal upper region, only S relative abundance was affected by decreasing in response to infection in *R. microplus* (Fig. 2).

As reported here in ticks, the presence of N, C, O, P, Cl and K was previously identified in the jewel beetle *Pseudo Taenia frenchie* mandible [4]. Although at least part of the Al may be a contamination from the aluminum scanning electron microscope stubs, herein we provided the first evidence for the presence of the post-transition metal Al in tick exoskeleton. As found here in ticks, the presence of certain elements such as Si is rare in arthropod exoskeleton [6].

Chemical elements such as Cl, together with Al and Mg may contribute to exoskeleton biomineralization of protein components and coating [6,7]. The structural proteins described in arthropod exoskeleton and cytoskeleton include keratins and desmoplakin [8,9], which are involved in biomineralization processes [10,11]. The structural proteins in blood-feeding arthropods such as ticks may derive from both host and ectoparasite and the levels of tick and host derived proteins vary in response to pathogen infection [12–15]. As an example, the analysis by immunofluorescence in the salivary glands of *A. phagocytophilum*-infected and uninfected *I. scapularis* of pan-keratin (average  $\pm$  S.D. CTF-FITC, 4100  $\pm$  900 infected, 1050  $\pm$  120 control) and desmoplakin (average  $\pm$  S.D. CTF-FITC, 3800  $\pm$  750 infected, 950  $\pm$  140 control) showed over-representation (3.9-fold and 4.0-fold for pan-keratin and desmoplakin, respectively; *p* < 0.05) in infected ticks (Fig. 3A and B). These proteins may affect directly or indirectly the composition of the exoskeleton through biomineralization with some of the chemical elements found in ticks. The atomic composition in host and tick derived pan-keratin and desmoplakin proteins positively correlated with *I. scapularis* exoskeleton composition in both infected and control ticks (Table 1) suggesting that structural proteins directly affect the chemical composition of tick exoskeleton. However, due to the finding that the composition of some of these chemical elements increased or decreased while representation for both proteins increased in response to infection suggested that factors different from protein levels may affect chemical composition of the exoskeleton between infected and uninfected ticks.

The results of this study provided evidences showing that tick exoskeleton contains chemical elements also found in other arthropods. Some of the identified elements such as Mg and Al may be involved in tick exoskeleton stabilization through biomineralization of structural proteins that may be overrepresented in response to pathogen infection. These results suggested that pathogen infection alters the chemical composition of tick

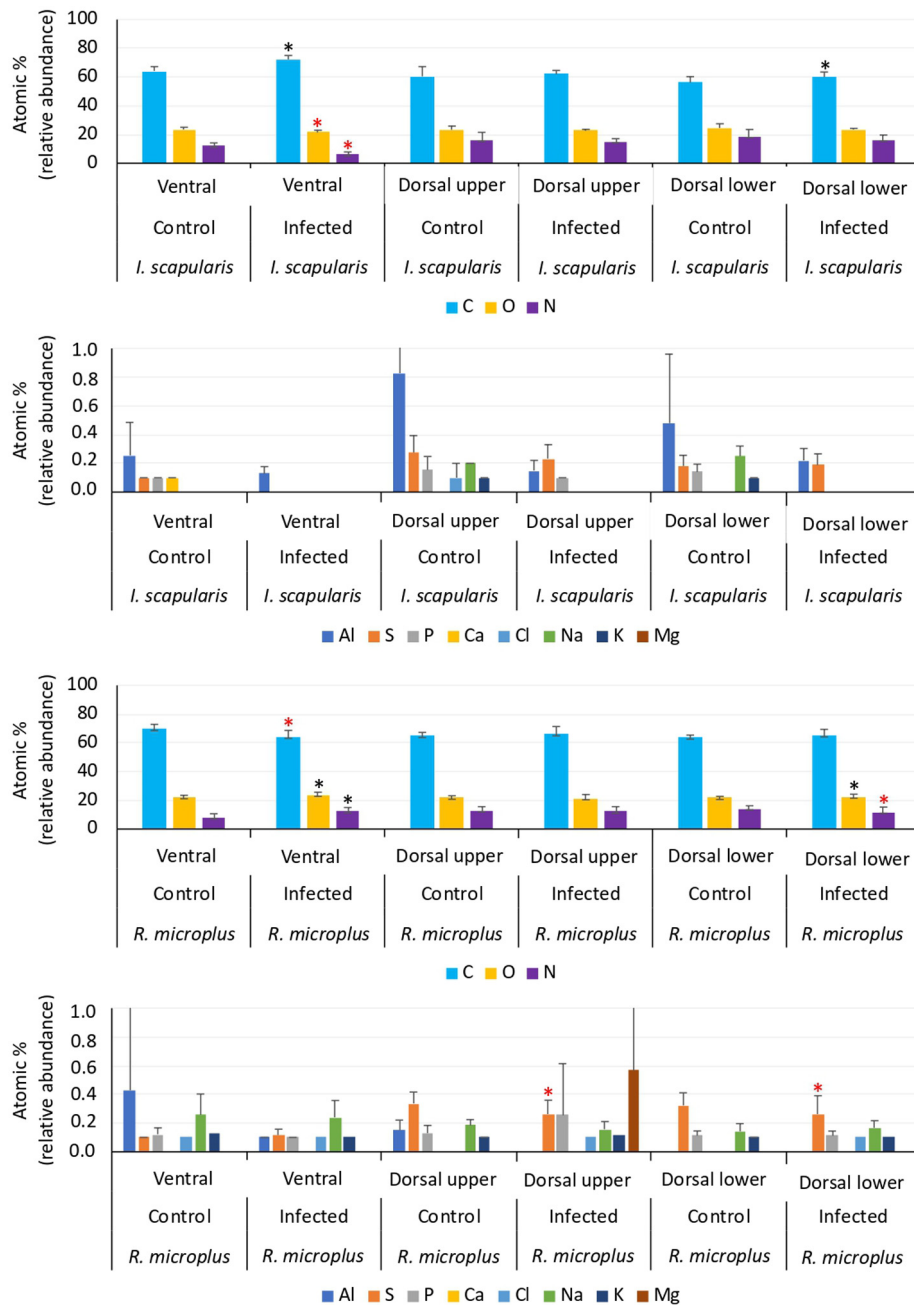


**Fig. 2.** Effect of pathogen infection on the relative abundance of chemical elements in tick exoskeleton. Chemical elements with high relative abundance (C, O and N with >10 at.%) and low relative abundance (<1 at.%) were represented as average + SD for each tick species (*I. scapularis* and *R. microplus*) and exoskeleton region (ventral, dorsal upper and dorsal lower) and compared between infected and uninfected control ticks by Student's *t*-test with unequal variance and one-way ANOVA test ( $p < 0.05$ ,  $N = 6$  biological replicates and 9 analyses per replicate). Only values with statistically significant differences by both test analyses were considered (\* $p < 0.05$ ; in black for augmented and in red for decreased elements in response to infection). (For interpretation of the references to colour in this figure legend, the reader is referred to the web version of this article.)

exoskeleton by mechanisms still to be characterized and with tick species and exoskeleton region-specific differences. Differences between tick species were recently reported for the mechanical properties of tick cuticle [16]. These mechanisms may be part of the conflict and cooperation evolutionary relationship between ticks and pathogens [17]. However, differences in the chemical composition of tick exoskeleton may be also affected by host blood meal, which may vary in response to pathogen infection and between different individuals and host species. Although still preliminary, these results suggested the possibility of using

elementomics approaches [18] for characterizing and targeting metabolic pathways and proteins in the exoskeleton for the control of tick infestations and pathogen infection [19,20].

### 3. Methods

#### 3.1. Ticks

The *I. scapularis* ticks were obtained from the laboratory colony maintained at the Oklahoma State University Tick Rearing Facility.

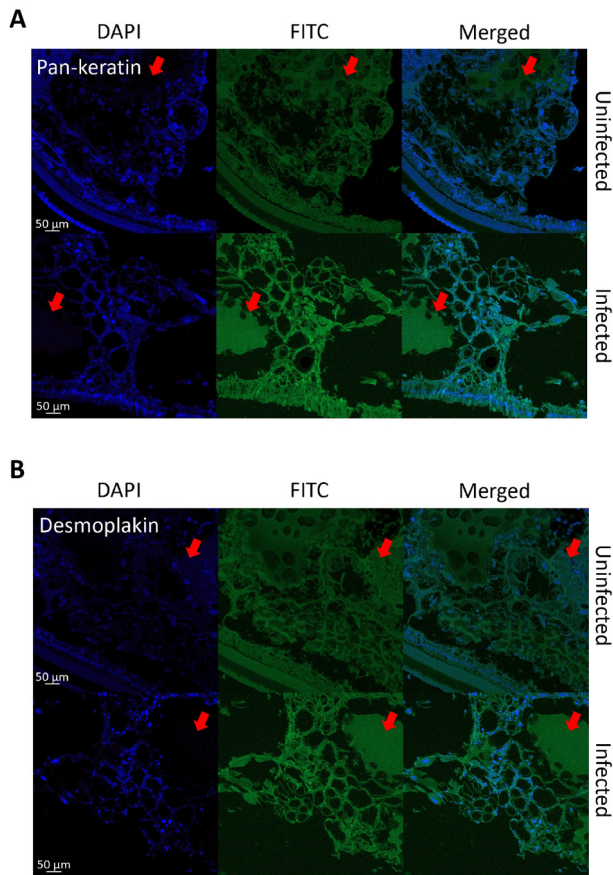


**Fig. 3.** Example of changes in the levels of structural proteins in response to pathogen infection in ticks. Representative images of immunofluorescence analysis of salivary glands in uninfected and *A. phagocytophilum*-infected adult female *I. scapularis*. Tick tissues were incubated with (A) anti-pan-keratin and (B) anti-desmoplakin antibodies. The green channel is the protein stained with goat anti-rabbit IgG-FITC antibodies. The blue channel is DAPI-stained DNA (nucleus). Merge is a merged image of green and blue channels. Red arrows show deposits of these proteins with higher levels in infected samples. Scale bar: 50  $\mu\text{m}$ . (For interpretation of the references to colour in this figure legend, the reader is referred to the web version of this article.)

**Table 1**  
Atomic composition of structural proteins and correlation with tick *I. scapularis* exoskeleton.

Sample	Atomic composition formula	Spearman's Rho $r_s$ , p
<i>Tick</i>		
Desmoplakin	C <sub>12229</sub> H <sub>19622</sub> N <sub>3658</sub> O <sub>3853</sub> S <sub>56</sub>	
Pan-keratin	C <sub>311</sub> H <sub>453</sub> N <sub>89</sub> O <sub>84</sub> S <sub>5</sub>	
Desmoplakin + pan-keratin	C <sub>12540</sub> H <sub>20075</sub> N <sub>3747</sub> O <sub>3937</sub> S <sub>61</sub>	
Control tick exoskeleton	C <sub>60</sub> N <sub>16</sub> O <sub>24</sub> S <sub>0</sub>	$r_s = 1$ , p = 0
Infected tick exoskeleton	C <sub>65</sub> N <sub>13</sub> O <sub>22</sub> S <sub>0</sub>	$r_s = 1$ , p = 0
<i>Sheep</i>		
Desmoplakin	C <sub>13789</sub> H <sub>22517</sub> N <sub>4017</sub> O <sub>4401</sub> S <sub>90</sub>	
Pan-keratin	C <sub>1961</sub> H <sub>3173</sub> N <sub>579</sub> O <sub>650</sub> S <sub>25</sub>	
Desmoplakin + pan-keratin	C <sub>15750</sub> H <sub>25690</sub> N <sub>4596</sub> O <sub>5051</sub> S <sub>115</sub>	
Control tick exoskeleton	C <sub>60</sub> N <sub>16</sub> O <sub>24</sub> S <sub>0</sub>	$r_s = 1$ , p = 0
Infected tick exoskeleton	C <sub>65</sub> N <sub>13</sub> O <sub>22</sub> S <sub>0</sub>	$r_s = 1$ , p = 0

The atomic composition of tick and sheep derived pan-keratin and desmoplakin was analyzed using the ProtParam tool (<https://web.expasy.org/protparam>). A Spearman's Rho correlation (<https://www.socscistatistics.com/tests/spearman/default2.aspx>) analysis between total tick or sheep (pan-keratin + desmoplakin) protein atomic composition and chemical atomic % of relative abundance of tick exoskeleton in *I. scapularis* infected and control ticks using the elements identified in both proteins and tick exoskeleton (C, N, O, S).

Larvae and nymphs were fed on rabbits and adults were fed on sheep. Adult female ticks were infected with *A. phagocytophilum* as previously described [13] by feeding on a sheep inoculated intravenously with approximately  $1 \times 10^7$  *A. phagocytophilum* (NY18 isolate)-infected HL-60 cells (90–100% infected cells). Control ticks were fed on uninfected sheep. Fully engorged infected and uninfected engorged female ticks were collected for analysis. Animals were housed and experiments conducted with the approval and supervision of the OSU Institutional Animal Care and Use Committee (Animal Care and Use Protocol, ACUP No. VM1026). The *R. microplus* (susceptible Media Joya strain, CENAPA, Mexico) ticks were obtained from a laboratory colony maintained at the University of Tamaulipas, Mexico [21]. Tick larvae were fed on cross-bred *Bos taurus* cattle and collected after repletion to allow for oviposition and hatching in humidity chambers at 12 h light:12 h dark photoperiod, 22–25 °C and 95% relative humidity (RH). Larvae were used for infestations at 15 days after hatching from eggs. Ticks were infected with *A. marginale* by feeding on naturally infected cattle as previously reported [21]. Control ticks were fed on uninfected cattle. Infected and uninfected fully engorged female ticks were collected for analysis. The study was conducted in accordance with standards specified in the Guide for Care and Use of Laboratory Animals for the University of Tamaulipas (UAT), Mexico. The protocol was approved by the ethics committee of the UAT (No. CBBA\_17\_0). Collected *I. scapularis* and *R. microplus* ticks were washed as previously described [22] and stored in 70% ethanol until analysis.

### 3.2. Scanning electron microscopy and energy dispersive spectroscopy analysis

Female ticks were dehydrated in an incubator at 37 °C for 24 h as a preparation for scanning electron microscopy (SEM) photography. Specimens were properly placed and mounted onto standard aluminum SEM stubs using conductive carbon adhesive tabs. Ticks were observed and photographed with a field emission scanning electron microscope (Zeiss GeminiSEM 500, Oberkochen, Germany) operating in high vacuum mode at an accelerating voltage of 2 kV and with no metallic coating. Elemental composition of the tick exoskeleton dorsal upper, dorsal lower and ventral regions (Fig. 1A) were determined with 3 scans on each exoskeleton region using an energy dispersive spectroscopy (EDS) 80 mm<sup>2</sup> detector at 15 kV (Oxford Instruments, Abingdon, United Kingdom). Results were compared between infected and uninfected control ticks by Student's *t*-test with unequal variance and one-way ANOVA test (<https://www.socscistatistics.com/tests/anova/default2.aspx>) ( $p < 0.05$ , N = 6 biological replicates and 9 analyses per replicate). The results are displayed in Table S1 and Data S1.

### 3.3. Immunofluorescence assay

Female *I. scapularis* ticks fed on *A. phagocytophilum*-infected and uninfected sheep and fixed with 4% paraformaldehyde in 0.2 M sodium cacodylate buffer were embedded in paraffin and used to prepare sections on glass slides as previously described [13]. The paraffin was removed from the sections with xylene and then hydrated by successive 2 min washes with a graded series of 100, 95, 80, 75, and 50% ethanol. The slides were treated with Proteinase K (Dako, Barcelona, Spain) for 7 min, washed with PBS and incubated with 3% BSA (Sigma-Aldrich) in PBS for 1 h at RT. Then the slides were incubated with antibodies against desmoplakin (ab106342) and pan-keratin (ab190625) (Abcam, Cambridge, UK) diluted 1:100 in 3% BSA/PBS for 14 h at 4 °C. After additional washes in PBS, the sections were incubated with FITC conjugated goat anti-rabbit IgG secondary antibodies (Sigma-Aldrich), diluted 1:80 in 3% BSA/PBS, for 1 h at RT. Finally, the slides were mounted

using Prolong Gold antifade reagent with DAPI reagent (Molecular Probes, Eugene, OR, USA). The slides were examined using a Zeiss LSM 800 laser scanning confocal microscope (Carl Zeiss, Oberkochen, Germany) with a 10× objective. Sections incubated with pre-immune serum were used as controls. Using ImageJ, an outline was drawn around each area, mean fluorescence and integrated density were measured, along with several adjacent background readings. Then, the total corrected tissue fluorescence (CTF) was calculated as integrated density – (area of selected tissue × mean fluorescence of background readings) [23] and compared between infected and uninfected cells by Student's *t*-test with unequal variance ( $p = 0.05$ ;  $N = 4$ –6 biological replicates).

#### 3.4. Atomic composition of structural proteins

The atomic composition of pan-keratin and desmoplakin was analyzed using the ProtParam tool (<https://web.expasy.org/protparam>). The correlation analysis between total (pan-keratin + desmoplakin) protein atomic composition for both tick (B7QA44\_IXOSC, A0A4D5S190\_IXOSC) and sheep (K1M2\_SHEEP, W5Q7Z7\_SHEEP) derived proteins and chemical atomic% of relative abundance of tick exoskeleton in *I. scapularis* infected or control ticks was performed using the elements identified in both proteins and tick exoskeleton (C, N, O, S) with Spearman's Rho calculator (<https://www.socscistatistics.com/tests/spearman/default2.aspx>).

#### Declaration of Competing Interest

The authors declare that they have no known competing financial interests or personal relationships that could have appeared to influence the work reported in this paper.

#### Acknowledgments

We thank Alberto Moraga Fernández (IREC, Spain) for assistance with tick analysis. This research was partially supported by the Consejería de Educación, Cultura y Deportes, JCCM, Spain, project CCM17-PIC-036 (SBPLY/17/180501/000185).

#### Appendix A. Supplementary data

Supplementary data to this article can be found online at <https://doi.org/10.1016/j.csbj.2020.01.003>.

#### References

- [1] Jongejans F, Uilenberg G. The global importance of ticks. *Parasitology* 2004;129: S3–S14.

- [2] de la Fuente J, Estrada-Peña A, Venzal JM, Kocan KM, Sonenshine DE. Overview: ticks as vectors of pathogens that cause disease in humans and animals. *Front Biosci* 2008;13:6938–46.
- [3] Flynn PC, Kaufman WR. Mechanical properties of the cuticle of the tick *Amblyomma hebraeum* (Acari: Ixodidae). *J Exp Biol* 2015;218:2806–14.
- [4] Cribb BW, Lin CL, Rintoul L, Rasch R, Hasenpusch J, Huang H. Hardness in arthropod exoskeletons in the absence of transition metals. *Acta Biomater* 2010;6:3152–6.
- [5] Gallant JG, Hochberg R, Ada E. Elemental characterization of the cuticle in the pseudoscorpion *Halobisium occidentale*. *Invert Biol* 2016;135:127–37.
- [6] Gallant J, Hochberg R. Elemental characterization of the exoskeleton in the whipscorpions *Mastigoproctus giganteus* and *Typopeltis dalyi* (Arachnida: Thelyphonida). *Invertebr Biol* 2017;136:345–59.
- [7] Suppan J, Engel B, Marchetti-Deschmann M, Nürnberger S. Tick attachment cement—reviewing the mysteries of a biological skin plug system. *Biol Rev Camb Philos Soc* 2018;93:1056–76.
- [8] Robinson Jr GR, Sibrell PL, Boughton CJ, Yang LH. Influence of soil chemistry on metal and bioessential element concentrations in nymphal and adult periodical cicadas (*Magicicada* spp.). *Sci Total Environ* 2007;374:367–78.
- [9] Delva E, Tucker DK, Kowalczyk AP. The desmosome. *Cold Spring Harb Perspect Biol* 2009;1:a002543.
- [10] Blakey PR, Earland C, Stell JGP. Calcification of keratin. *Nature* 1963;198:481.
- [11] Checa AG, Salas C, Harper EM, Bueno-Pérez J de D. Early stage biomineralization in the periostracum of the 'living fossil' bivalve *Neotrigonia*. *PLoS One* 2014;9:e90033.
- [12] Kim TK, Tirloni L, Pinto AF, Moresco J, Yates 3rd JR, da Silva Jr Vaz I, et al. *Ixodes scapularis* tick saliva proteins sequentially secreted every 24 h during blood feeding. *PLoS Negl Trop Dis* 2016;10:e0004323.
- [13] Ayllón N, Villar V, Galindo RC, Kocan KM, Šima R, López JA, et al. Systems biology of tissue-specific response to *Anaplasma phagocytophilum* reveals differentiated apoptosis in the tick vector *Ixodes scapularis*. *PLoS Genet* 2015;11:e1005120.
- [14] Villar M, López V, Ayllón N, Cabezas-Cruz A, López JA, Vázquez J, et al. The intracellular bacterium *Anaplasma phagocytophilum* selectively manipulates the levels of vertebrate host proteins in the tick vector *Ixodes scapularis*. *Parasit Vectors* 2016;9:467.
- [15] Laskay UA, Brei L, Vilcins IM, Dietrich G, Barbour AG, Piesman J, et al. Survival of host blood proteins in *Ixodes scapularis* (Acari: Ixodidae) ticks: a time course study. *J Med Entomol* 2013;50:1282–90.
- [16] Kaufman WR, Flynn PC. A comparison of the cuticular properties of the female ticks *Ixodes pacificus* and *Amblyomma hebraeum* (Acari: Ixodidae) throughout the feeding period. *Exp Appl Acarol* 2018;76:365–80.
- [17] de la Fuente J, Villar M, Cabezas-Cruz A, Estrada-Peña A, Ayllón N, Alberdi P. Tick-host-pathogen interactions: conflict and cooperation. *PLoS Pathog* 2016;12:e1005488.
- [18] Li Y-F, Chen C, Qu Y, Gao Y, Li B, Zhao Y, et al. Metallomics, elementomics, and analytical techniques. *Pure Appl Chem* 2008;80:2577–94.
- [19] Spindler KD, Spindler-Barth M, Londershausen M. Chitin metabolism: a target for drugs against parasites. *Parasitol Res* 1990;76:283–8.
- [20] You M, Fujisaki K. Vaccination effects of recombinant chitinase protein from the hard tick *Haemaphysalis longicornis* (Acari: Ixodidae). *J Vet Med Sci* 2009;71:709–12.
- [21] Merino O, Almazán C, Canales M, Villar M, Moreno-Cid JA, Galindo RC, et al. Targeting the tick protective antigen subolesin reduces vector infestations and pathogen infection by *Anaplasma marginale* and *Babesia bigemina*. *Vaccine* 2011;29:8575–9.
- [22] Kocan KM, Blouin E, de la Fuente J. RNA interference in ticks. *J Vis Exp* 2011;47: e2474.
- [23] Parry WL, Hemstreet 3rd GP. Cancer detection by quantitative fluorescence image analysis. *J Urol* 1988;139:270–4.